XPS and Raman studies of electron irradiated sodium silicate glass

Chen Liang(陈 亮), Wang Tie-Shan(王铁山)†, Zhang Gen-Fa(张根发),
Yang Kun-Jie(杨坤杰), Peng Hai-Bo(彭海波), and Zhang Li-Min(张利民)

School of Nuclear Science and Technology, Lanzhou University, Lanzhou 730000, *China*

(Received 3 January 2013; revised manuscript received 31 May 2013)

The microstructure modifications of sodium silicate glass induced by 1.2-MeV electron irradiation are studied by x-ray photoelectron spectroscopy and Raman spectroscopy. Depth profile analyses are also performed on the irradiated glass at 10^9 Gy. A sodium-depleted layer with a thickness of a few tens of nanometers and the corresponding increase of network polymerization on the top surface are observed after electron bombardment, while the polymerization in the subsurface region has a negligible variation with the irradiation dose. Moreover, the formation of molecular oxygen after electron irradiation is evidenced, which is mainly aggregated in the first two-micron-thick irradiated glass surface. These modifications are correlated to the network relaxation process as a consequence of the diffusion and desorption of sodium species during electron irradiation.

Keywords: silicate glass, electron irradiation, network polymerization, oxygen molecule

PACS: 61.43.Fs, 61.80.Fe **DOI:** 10.1088/1674-1056/22/12/126101

1. Introduction

Silicate glass is widely used in technologies, such as the light emitting diode, the microelectromechanical system, and the space shuttle.[1–3] Understanding the structural evolution under irradiation is crucial for its basic and advanced technological applications, especially for evaluating its performance after long-term interactions with the irradiation environment.

Typical silicate glass is composed of the SiO_4 tetrahedrons sharing all four corner oxygen atoms to form a continuous three-dimensional (3D) network.[1] The oxygen at the corner is bridging two silicon atoms and is called bridging oxygen (BO), which can be described as ≡Si–O–Si≡. When an alkali oxide, for example Na_2O, is added into the silicate glass, the introduced Na^+ partly destroys the network to form a non-bridging oxygen (NBO) atom, which can be described as ≡Si–O^-Na^+. Each NBO is associated with a nearby Na^+ to maintain the local charge neutrality. The structure can be viewed as a network of silicon–oxygen tetrahedron with occasional breaks in connectivity due to the NBO. The connectivity accounts for the framework disorder, which describes the distribution of SiO_4 units alone, and the degree of polymerization, that refers to mixing between SiO_4 and Na cations, controlling the distribution of NBO.[4] To describe the polymerization of the network structure in silicate, the silicate tetrahedrons are classified as Q^n species, where the Q^n species refers to the SiO_4 tetrahedral units with n BO atoms. For example, a Q^2 species has two bridging and two non-bridging oxygen atoms. The four major SiO_4 tetrahedral units respectively with one, two, three, and four BOs are given in Fig. 1. As shown in Fig. 1, the Na^+ ion is rather weakly bounded to the NBO. The migration of Na^+ is responsible for the structural evolution during electron irradiation.[5–12]

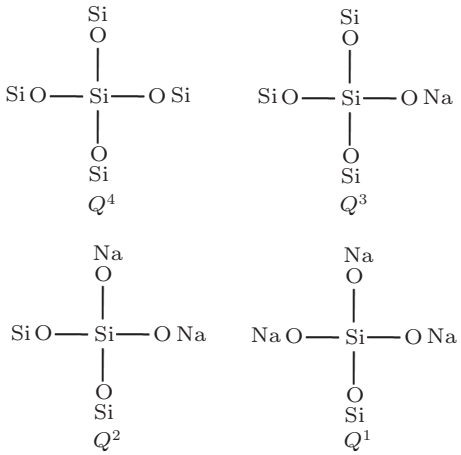


Fig. 1. SiO_4 tetrahedral units respectively with one, two, three and four non-bridging oxygens.

Depending on the electron energy and irradiation dose, the microstructure changes including defect creation,[6,7] polymerization,[8,9] O_2 molecule/bubble formation,[10,11] and phase separation[11,12] have been reported. The most prominent effect concerns the migration of alkali ions, which has been well observed by Auger electron spectroscopy (AES) and electron probe microanalysis (EPMA).[13–15] The local surface concentration and depth distribution of alkali species can be changed during electron irradiation. Alkali ions are released from their initial sites and are driven by the electric field towards the bulk, which is referred to as a negatively charged layer formed by trapping incoming electrons at about the electron penetration depth. Moreover, there also exists an electron-stimulated desorption of alkali metal species during electron irradiation,[13] which has been explained on the basis

†Corresponding author. E-mail: tswang@lzu.edu.cn

© 2013 Chinese Physical Society and IOP Publishing Ltd

of Gibbsian segregation.[14] The segregation provides a driving force for the diffusion and desorption of alkali species and thus forms a depletion zone beneath the surface.

Accompanied with migration of alkali ions, the oxygen molecule can be formed as a consequence of rebinding the glass network, thus causing significant modifications to the composition and properties of the glass sample. However, to our knowledge, very few studies have been carried out on the analysis of the composition and microstructure of irradiated multicomponent glass in depth. Although Ollier *et al*.[9] have studied the O_2 formation in irradiated glass by Raman depth profile, which showed O_2 formation and aggregation at surface after electron irradiation, nevertheless, the irradiation effects are strongly dependent on the structure, bonding, and composition of the glass sample. The micromechanisms of O_2 aggregation and the corresponding modifications to polymerization caused by the migration of alkali ions are still not yet well understood.

In this paper, we extensively consider these phenomena, concerning modifications to polymerization and the formation of molecular oxygen varying the depth of irradiated glass, which are associated with diffusion and desorption of sodium species. Based on our experimental results, the process of electron interaction with glass and the subsequent network relaxation process are discussed.

2. Experiment

A commercial sodium silicate glass with compositions 70±5 wt% SiO_2, 17±3 wt% Na_2O, 5.5±1.5 wt% Al_2O_3, 4.5±1.5 wt% B_2O_3, 4±1 wt% CeO_2, and minor ZnO + SrO was used in this study. The sample, with a size of 5 mm×5 mm×0.5 mm, was fine polished and ultrasonically cleaned prior to electron irradiation. The irradiation was performed using electrons generated by a high voltage transformer type electron accelerator operating at 1.2 MeV and 15 mA, in the national laboratory of the heavy ion accelerator research facility, Lanzhou (HIRFL). The homogeneous irradiation of the glass sample was obtained in these conditions of sample thickness and beam conditions.[16] Different doses from 5×10^6 Gy to 10^9 Gy were used and the samples were cooled by water during the irradiation experiment.

The x-ray photoelectron spectroscopy (XPS) spectra were measured on an x-ray photoelectrometer (K-Alpha-surface Analysis, Thermon Scientific) equipped with x-ray monochromatisation, which provides information about the bonding environment and elemental composition of top surface layers (up to 10 nm). Integrated areas of XPS transitions were determined following Shirley's inelastic background subtraction method.[17] The experimental uncertainties accompanied with an XPS quantitative analysis were estimated to be 5%. The O 1s XPS signals were fitted with mixed Gaussian–Lorentzian curves (G–L ratio = 30%).[18] A charge shift in the binding energy of typically 1 eV∼2 eV was observed for the samples due to surface charging. The shift was corrected by measuring the C 1s peak, which was assumed to be 284.8 eV. Depth-profiling was also employed using 3-keV Ar^+ sputtering to quantify the chemical composition as a function of the depth. When the effects of Ar ion sputtering on the samples are considered,[19] XPS spectra were also measured on the pristine sample for the same sputtering time.

The Raman spectra were obtained on a Labram HR 800 micro-spectrometer using the 532-nm line of an argon ion laser at 100 mW. The experiments were carried out with a confocal ×100 objective. Under our experimental conditions, the optical penetration depth of the Raman excitation light was about 1 μm.[20] The spectrometer resolution was approximately 1 cm^{-1}. The Raman depth profile experiments were carried out by acquiring Raman spectra from the surface to the inside of the glass in steps of 1 μm for z-displacement along a fixed horizontal position.

3. Results and discussion

3.1. XPS spectrum analysis

Figure 2 shows the core-level spectra in the O 1s region for the pristine and electron irradiated glasses. As shown in the figures, the O 1s spectra are shifted toward higher binding energy. This shift is approximately 1 eV after electron irradiation at 10^9 Gy, which correlates with the reduction of the sodium content in the glass surface after irradiation.[21] The O 1s peak fit indicates two different bonding states of oxygen in the pristine glass, which can be assigned to the BO and NBO bond, respectively.[18,21] The sodium silicate glass studied in this paper should have various bridging and non-bridging bondings, such as Si–O–Si, B–O–B, Al–O–Al, Si–O–B, Si–O–Al, Si–O–Na, B–O–Na, and Al–O–Na. However, as the FWHMs of the BO (1.69 eV) and NBO (1.99 eV) components are so small, it is impossible to evaluate the validity of the further separation by three or more components. In addition, the sodium silicate glass studied in this paper only has a minor content of B_2O_3 and Al_2O_3 compared with the SiO_2 content, the contributions to the bridging and non-bridging bonding seem to be insignificant. The peak ratio of NBO to BO component reaches about 0.35±0.05 for the pristine glass surface and decreases with the increase of irradiation dose, which indicates an increase of the network polymerization. As shown in Fig. 2(c), the NBO component cannot be resolved after electron irradiation at 10^9 Gy, corresponding to the fact that a fully polymerized network is formed in the top surface layers.

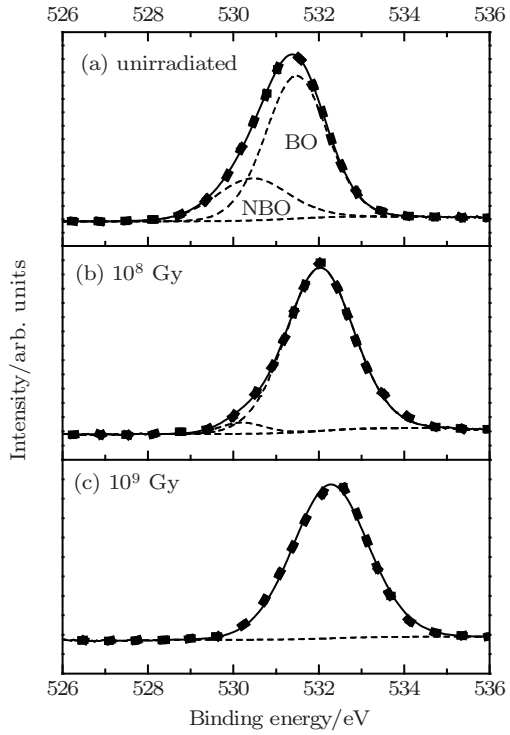


Fig. 2. Comparison of O 1s spectra between the pristine and irradiated glasses. The dot lines denote the experimental data, the solid lines and dashed lines refer to the results of curve fitting.

The NBO is very closely related to sodium atoms. The fully polymerized network is thus corresponding to the depletion of the sodium content, which is evidenced by the sodium concentration profile obtained in the XPS depth profile on the electron irradiated glass at 10^9 Gy. As shown in Fig. 3, almost no change on the pristine glass is observed except the small value on the top surface ($t = 0$ min), which can be attributed to contamination (mainly carbon and nitrogen contamination) on the surface. Nevertheless, the sodium content is almost completely depleted in the top surface layers of irradiated glass, which is consistent with the formation of a fully polymerized network. The value gradually increases with the depth of irradiated glass increasing and reaches the pristine value after etching for about 40 min. When the etching rate is about 1 nm/min,[22] the sodium depleted layer is around 40-nm thick. The formation of a sodium depleted layer may be referred to as both the electric field enhanced diffusion and the electron stimulated desorption (ESD) of sodium as a consequence of electron irradiation.[13]

When high-energy electrons penetrate the glass sample, the $[\text{Si-NBO}]^+$ and Na^+ ion pairs can be created in the whole volume through double ionization processes.[12] The attractive electrostatic force between the NBO and Na is turned into a repulsive one, thus causing a positive charge in the glass sample. As electrical equilibrium cannot be quickly restored on the atomic scale in the glass by electrons coming from the surroundings, the sodium ion is no longer rigidly bonded to the oxygen and can be driven either to diffuse to an interstitial site if it is in the bulk or be desorbed into the vacuum if it is on the surface. The diffusion is closely related to the distribution of the electric field induced by electron irradiation. It should be noted that the charge distribution generated by penetration of a high-energy electron can be considered as being uniform,[23] except a stronger repulsive interaction on the top layers induced by the emission of secondary electrons.[23,24] Therefore, the diffusion of sodium ions can be considered as being homogeneous, instead of only diffusion following one direction driven by an electric field formed by the trapped electrons inside the sample.[14,15] The electron stimulated desorption (ESD) of sodium can also occur in the case of repulsive interactions between the sodium species and the surface. Several physical mechanisms have been suggested to explain ESD phenomena from different types of surfaces.[25] ESD can be viewed as a multiple-step process involving electronic excitation of surface species followed by the escape of an excited fragment out of the surface. The desorbed species include ions and excited neutrals, but in most cases the cross sections for neutral desorption are larger.[25,26] Once the desorption has occurred within the outermost layer, an activity concentration gradient exists to drive the out-diffusion of sodium liberated by the double ionization process in the subsurface.

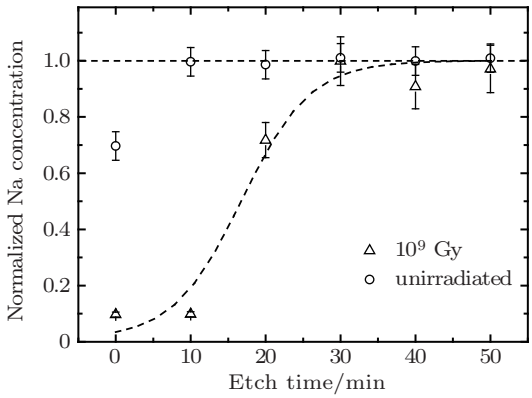


Fig. 3. Variations of normalized Na concentration with depth in the pristine and irradiated glasses. The dashed lines are guides for the eyes.

3.2. Raman spectrum analysis

The formation of oxygen molecule (O_2) after electron irradiation is observed in our Raman results. As shown in Fig. 4, a narrow peak appears at around 1550 cm^{-1} in the Raman spectrum of electron irradiated glass at 10^9 Gy, which corresponds to the stretching vibration mode of the O–O bond in the oxygen molecule. This result is consistent with previous Raman results,[8,9] which suggests that the diffusion of sodium ions during electron irradiation is responsible for this structural evolution on sodium silicate glass.

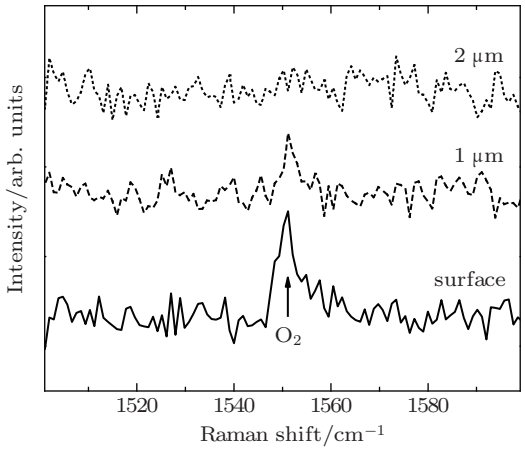


Fig. 4. Raman spectra in the 1500 cm^{-1}∼1600 cm^{-1} region of irradiated glass at 10^9 Gy.

The remaining loose structure caused by the diffusion of the sodium wound tends to pull itself together and recombine into relaxed SiO_4 units. During the relaxation processes, the dangling bond on NBO may attract a neighboring NBO and form a peroxide bond (Si–O–O–Si).[12] However, the peroxide bond may quickly go towards the relaxed Si–O–Si configuration, thereby facilitating migration of sodium ions through percolation channels between large connected clusters of SiO_2 structurally relaxed units.[27] This process can be depicted as[12,27]

$$2(\equiv \mathrm{Si}-\mathrm{NBO}^0) \rightarrow \equiv \mathrm{Si}-\mathrm{O}-\mathrm{O}-\mathrm{Si} \equiv \rightarrow$$
$$\equiv \mathrm{Si}-\mathrm{O}-\mathrm{Si} \equiv +1/2\,\mathrm{O}_2. \quad (1)$$

This process will also cause locally oversaturated oxygen and then form molecular oxygen O_2, as confirmed by a peak arising that corresponds to the stretching vibration mode of the O–O bond in molecular oxygen O_2 after electron irradiation. O_2 is detected down to 2 μm from the top surface; the concentration is lower in depth than in surface. It indicates that O_2 is diffused into the surface through the same percolation channels between large SiO_2 relaxed units as sodium diffusion, without influencing the sodium depleted layer. This result is similar to the result from a previous Raman depth profile study,[9] where the molecular oxygen thickness in the layer is less than 15 μm. However, the oxygen enriched layer is much thinner in our result. As the formation of the O_2 layer is correlated to the migration of alkali ions, the distinction can be attributed to the Ce content (4±1 wt% CeO_2) in our glass sample, which could reduce the migration rate of alkali ions through reducing the defect precursor.[7]

The modification on the polymerization of the network structure after electron irradiation is characterized by extracting out the Raman spectra between 850 cm^{-1}∼1320 cm^{-1} and then fitting with three Gaussian peaks: 980 cm^{-1} (Q^2), 1080 cm^{-1} (Q^3), 1150 cm^{-1} (Q^4), respectively.[28] The contribution from the Q^1 unit is negligible for the glass networks, which is usually centered near 910 cm^{-1}. Figure 5 shows an example of the Q^n species band deconvolution for the pristine sample. The relative area of each Q^n species makes it possible to calculate the fraction of NBO. Based on the Raman study of alkali silicate glass, the bulk NBO/Si ratio, and NBO/(BO + NBO) ratio were previously calculated.[29,30] In order to compare with the XPS results shown in Fig. 2, the ratio of NBO to BO is derived based on the previous calculations; it can be calculated by the following formula:

$$\frac{\mathrm{NBO}}{\mathrm{BO}} = \frac{2Q^2 + Q^3}{2Q^2 + 3Q^3 + 4Q^4}, \quad (2)$$

the NBO/BO ratio is about 0.38±0.05, which is consistent with the value obtained from the XPS stoichiometric result (0.35±0.05). The variations of the different Q^n species with the irradiation dose are shown in Fig. 6(a). The Q^3 species increase with Q^2 and Q^4 species decreasing, which indicates that the Q^n species balance equation ($2Q^3 = Q^2 + Q^4$) is shifted to the left as the increase of irradiation dose. The variations of different Q^n species with the depth of irradiated glass at 10^9 Gy are presented in Fig. 6(b), which suggests that no significant difference exists in Q^n species between the surface Raman and subsurface Raman spectra. However, as shown in Fig. 7, the calculated NBO/BO ratio has a negligible variation, indicating that the polymerization of a glass network has no significant change after electron irradiation.

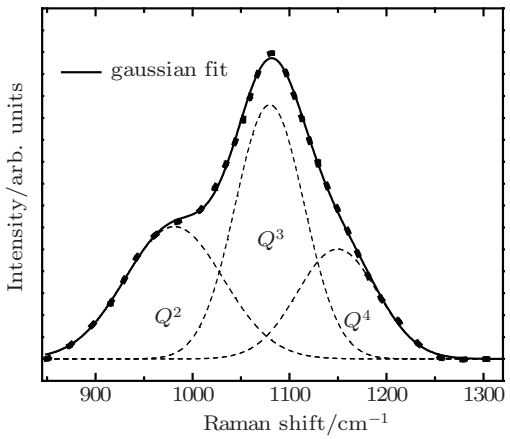


Fig. 5. Gaussian fits of Raman spectrum in the 850 cm^{-1}∼1320 cm^{-1} region of unirradiated glass.

However, the results of the negligible variation on the polymerization in Raman are inconsistent with our XPS results, as shown in Fig. 2, where the NBO/BO ratio decreases with the increase of irradiation dose. Nonetheless, it should be noted that there is a significant difference in the detected depth between XPS and Raman results, as illustrated in the experimental description. The Raman signal is detected in a range of several microns by surface Raman and Raman depth profile experiments, thus it can be considered representative of the subsurface region. Thus, the inconformity between the Raman

and XPS results suggests that the increase of network polymerization after electron irradiation occurs only in the top surface layers, without significant modification to the polymerization in the subsurface region.

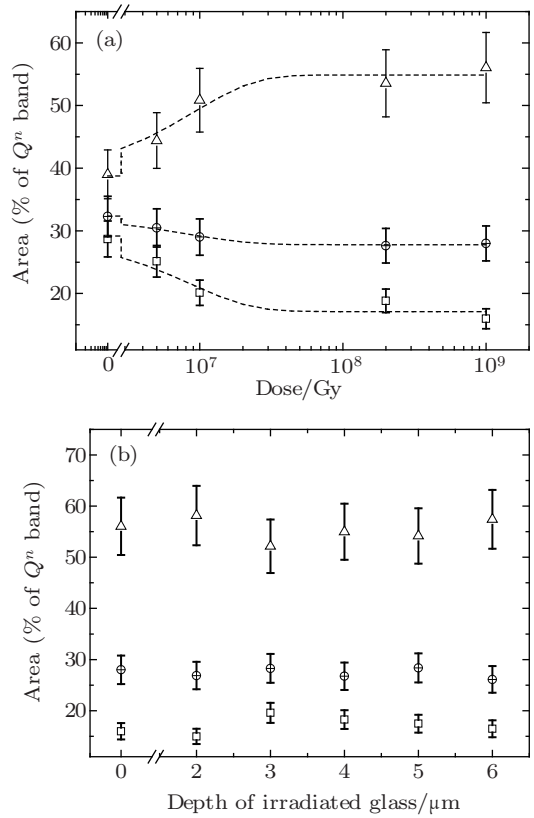


Fig. 6. Variations of Q^n species with dose (a) and depth (b) of irradiated glass at 10^9 Gy. Symbols ⊕, Δ, and □ represent Q^2, Q^3, and Q^4 species, respectively. The dashed lines are guides for the eyes.

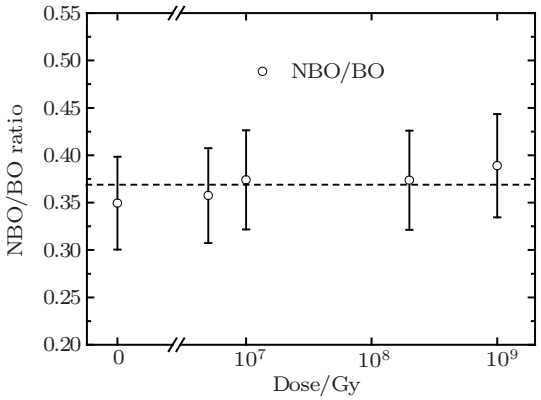


Fig. 7. Variation of the NBO/BO ratio with the dose. The dashed line is a guide for the eyes.

As some new species may be shown up (e.g. defects, molecular oxygen and so on) after electron irradiation, the glass network can be significantly modified, especially in the near-surface region. Due to the desorption of sodium species, the NBO bonds within the top surface region can be severely reduced after the network relaxation process, which is confirmed by XPS results, as shown in Fig. 2. In the subsurface region, modifications to the glass network are evidenced by variations of different Q^n species with the irradiation dose (Fig. 6). This result also suggests that diffusion of sodium ions does occur in the whole glass volume as a consequence of electron irradiation. Due to the diffusion of charge neutralized Na^+ around NBO, the dangling NBO bonds can be formed. The silicate network tries to maintain its structural continuity by the subsequent network relaxation processes. As we discussed above, during network relaxation, the rebinding of two neighboring dangling NBO atoms can reform the Si–O–Si bond (process 1). In addition, the released Na ion may also be attracted to a neighboring dangling NBO atom and recreates new NBO bonds.[31] Thus, the negligible variation in the polymerization of a glass network in the subsurface region can be considered as being almost totally recovered after network relaxation processes. The recovery process can be accomplished through the reformation of BO and NBO bonds during the relaxation of a glass network.

4. Conclusions

The effects of electron irradiation on sodium silicate glass are studied by x-ray photoelectron spectroscopy and Raman spectroscopy. As the significant difference in the detected depth between XPS and Raman spectra, modifications to both the surface and subsurface regions can be verified. Due to the desorption of sodium species, a distinctive surface with a sodium depleted layer and highly polymerized network appear. In the subsurface region, although transformation between different Q^n species and the formation of oxygen molecules are evidenced, the polymerization is almost fully recovered after the network relaxation process. The oxygen molecules are not influenced by the surface layer but they diffuse into the surface and mainly aggregate in the first two-micron-thick irradiated glass surface.

References

[1] Shelby J E 2005 *Introduction to Glass Science and Technology* (London: The Royal Society of Chemistry)
[2] Li C R, Xu W, Dong B, Li S F, Ding J H, Cheng Y Q and Yin H T 2010 *Chin. Phys. B* **19** 047801
[3] Tian H, Liu J W, Qiu K, Song J and Wang D J 2012 *Chin. Phys. B* **21** 098504
[4] Lee S K 2005 *Geochim. Cosmochim. Acta* **69** 3695
[5] Weber W J, Ewing R C, Angell C A, Arnold G W, Cormack A N, Delaye J M, Griscom D L, Hobbs L W, Navrotsky A, Price D L, Stoneham A M and Weinberg M C 1997 *J. Mater. Res.* **12** 1946
[6] Boizot B, Petite G, Ghaleb D and Calas G 1998 *Nucl. Instrum. Method B* **141** 580
[7] Malchukova E, Boizot B, Petite G and Ghaleb D 2007 *Phys. Stat. Sol.* **4** 1280
[8] Boizot B, Petite G, Ghaleb D, Reynard B and Calas G 1999 *J. Non-Crystal Solids* **243** 268
[9] Ollier N, Boizot B, Reynard B, Ghaleb D and Petite G 2005 *J. Nucl. Mater.* **340** 209
[10] Ollier N, Rizza G, Boizot B and Petite G 2006 *J. Appl. Phys.* **99** 073511
[11] Sun K, Wang L M, Ewing R C and Weber W J 2005 *Philos. Mag.* **85** 597
[12] Jiang N and Silcox J 2002 *J. Appl. Phys.* **92** 2310

[13] Ohuchi F and Holloway P H 1982 *J. Vac. Sci. Technol.* **20** 863
[14] Miotello A, Cinque G, Mazzoldi P and Pantano C G 1991 *Phys. Rev. B* **43** 3831
[15] Gedeon O, Jurek K and Hulinsky V 1999 *J. Non-Crystal Solids* **246** 1
[16] http://physics.nist.gov/PhysRefData/Star/Text/ESTAR.html
[17] Gedeon O and Zemek J 2003 *J. Non-Crystal Solids* **320** 177
[18] Mekki A, Holland D, McConville C F and Salim M 1996 *J. Non-Crystal Solids* **208** 267
[19] Brow R K 1988 *J. Non-Crystal Solids* **107** 1
[20] Bonfils J D, Peuget S, Panczer G, Ligny D D, Henry S, Noël P Y, Chenet A and Champagnon B 2010 *J. Non-Crystal Solids* **356** 388
[21] Miura Y, Kusano H, Nanba T and Matsumoto S 2001 *J. Non-Crystal Solids* **290** 1
[22] Henderson D O, George M A, Tung Y S, Mu R, Burger A, Morgan S H and Collins W E 1995 *J. Vac. Sci. Technol. A* **13** 1254
[23] Cazaux J 1986 *J. Appl. Phys.* **59** 1418
[24] Zhao S L and Bertrand P 2011 *Chin. Phys. B* **20** 037901
[25] Ramsier R D and Yates J T 1991 *Surf. Sci. Rep.* **12** 243
[26] Czanderna A W, Madey T E and Powell C J 2002 *Beam Effects, Surface Topography, and Depth Profiling in Surface Analysis* (New York: Kluwer Academic)
[27] Miotello A and Toigo F 1987 *Nucl. Instrum. Method B* **19/20** 934
[28] Manara D, GranDjean A and Neuville D R 2009 *Am. Mineral.* **94** 777
[29] Umesaki N, Takahashi M, Tatsumisago M and Minami T 1996 *J. Non-Crystal Solids* **205–207** 225
[30] Wang M, Cheng J, Li M and He F 2011 *Physica B* **406** 3865
[31] Zemek J, Jiricek P, Gedeon O, Lesiak B and Jozwik A 2005 *J. Non-Crystal Solids* **351** 1665